Available online at www.sciencedirect.com

ScienceDirect

Journal of the European Ceramic Society 27 (2007) 2665–2669

www.elsevier.com/locate/jeurceramsoc

Preparation and characterization of Ag-magadiite nanocomposites

Kiyoshi Ozawa[a,*], Fumio Iso[b], Yasuhiro Nakao[c], Zhenxiang Cheng[d], Hiroki Fujii[a], Masashi Hase[a], Hitoshi Yamaguchi[a]

[a] National Institute for Materials Science, 1-2-1 Sengen, Tsukuba, Ibaraki 305-0047, Japan
[b] Southern District Technology Support Center, Industrial Technology Center of Tochigi Prefecture, 950 Tenjin-Cho, Sano, Tochigi 327-0847, Japan
[c] Honda Engineering Co., Ltd., 6-1 Hagadai, Haga-Machi, Haga-Gun, Tochigi 321-3395, Japan
[d] Institute for Superconducting and Electronics Materials, University of Wollongong, New South Wales 2522, Australia

Received 13 October 2006; received in revised form 21 November 2006; accepted 2 December 2006
Available online 24 January 2007

Abstract

Well-defined Ag-magadiite nanocomposites were successfully prepared by an ion-exchange method using a silver ammine complex, $[Ag(NH_3)_2]NO_3$, as the starting material. These nanocomposites were found to have a structure in which Ag-nanoparticles consisting of a single-crystalline particle were well dispersed in the interlayer spaces of two types of magadiite materials: Na-magadiite ($H_{0.2}Na_{1.8}Si_{14}O_{29}\cdot 7.8H_2O$) and H-magadiite ($H_{1.4}Na_{0.6}Si_{14}O_{29}\cdot 3.9H_2O$). Such Ag-nanoparticles appear to be caused by heating $[Ag(NH_3)_2]^+$ ions incorporated into the interlayer spaces of the magadiite materials by ion exchange with Na^+ ions. Furthermore, in nanocomposites heated at 120 °C in air, Ag-nanoparticles show a relatively uniform particle size of 3–5 nm, whereas a heterogeneous enlargement of Ag-nanoparticles occurs when the temperature exceeds ~180 °C.

Keywords: Nanocomposites

1. Introduction

Nanoparticles are of interest for fundamental studies and diversified technical applications because of their size-dependent properties or highly active performance due to large surface areas. However, when pure nanoparticles are used alone, they present some common problems, e.g., agglomeration between nanoparticles.[1] To overcome agglomeration, preparation of nanocomposites based on clay compounds, in which nanoparticles are supported within the interlaminar spaces of clay and/or on its external surfaces, is one of the most effective solutions. Thus, over the past 2 decades, much attention has been given to such nanocomposites, especially based on montmorillonite.[2–4]

Magadiite was first found as a natural mineral in the deposits of Lake Magadi, Kenya by Eugster[5] in 1967. This material is a hydrous sodium silicate with a multilayered structure, similar to many other clay compounds; its chemical composition is reported as $Na_2Si_{14}O_{29}\cdot nH_2O$.[5–8] This magadiite is described as Na-magadiite to distinguish it from H-magadiite that will be referred to hereafter. Synthesis of Na-magadiite was reported by Fletcher and Bibby.[7] Lagaly et al.[6] reported that Na-magadiite reacts readily with dilute acids, exchanging its interlayer Na^+ for H^+ to produce the material of H-magadiite. However, the exact structure of magadiite remains unknown because no suitable single crystal for X-ray diffraction analysis has ever been obtained.

From a practical point of view, such magadiite materials have some significant advantages. First, the pure materials can be readily synthesized on a large scale. Second, the materials show a high cation exchange capacity and ready sorption of polar organic molecules into their interlayer spaces.[6] These properties make the magadiite materials useful for possible development in various kinds of nanocomposite studies. However, until now, only a limited number of studies have been reported on such nanocomposite materials.[6,9]

Recently, we successfully prepared Ag-magadiite nanocomposites based on two types of magadiite materials: Na-magadiite and H-magadiite. For these nanocomposites, it was found that Ag-nanoparticles consisting of a single-crystalline particle with

---

[*] Corresponding author. Tel.: +81 29 859 2456; fax: +81 29 859 2301.
E-mail address: OZAWA.Kiyoshi@nims.go.jp (K. Ozawa).

0955-2219/$ – see front matter © 2006 Elsevier Ltd. All rights reserved.
doi:10.1016/j.jeurceramsoc.2006.12.002

a relatively uniform particle size of 3–5 nm are well dispersed in the interlayer spaces of each magadiite material.

In this paper, we describe the preparation of these nanocomposites and their structural characterization and morphology.

2. Experimental

2.1. Material preparation

Na-magadiite was prepared by the hydrothermal reaction of a silica gel (Wakogel Q-63, Wako Pure Chemical Industries, Ltd., Japan) with aqueous NaOH. The chemicals were weighed for the molar ratio of SiO_2:NaOH:H_2O = 1:0.23:18.5, transferred to a Teflon-lined cylindrical reactor, sealed, and then hydrothermally reacted at 150 °C for 48 h. After reaction, the dispersions were filtered, and the remaining solids were washed with distilled water. Some of the Na-magadiite was then converted to H-magadiite by ion exchange with 0.5 M aqueous HCl. Each magadiite material was dried at 40 °C for 48 h in air and then used for the preparation of the following nanocomposite materials.

Ag-magadiite nanocomposites were prepared by soaking 1.5 g of each magadiite in 50 ml of aqueous 0.5 M $[Ag(NH_3)_2]NO_3$, for which the suspensions were controlled to pH 10.6 with aqueous NH_3 and then kept with stirring at 30 °C for 6 days. The chemical of $[Ag(NH_3)_2]NO_3$ was synthesized from $AgNO_3$ and aqueous NH_3 according to the previously reported method.[10] After soaking, the dispersions in the suspensions were filtered, thoroughly washed with distilled water, and then dried at 40 °C for 48 h to give the nanocomposite materials. The resulting materials were heated at various temperatures ranging from 40 to 700 °C in air.

2.2. Characterizations

The specific surface areas of Na- and H-magadiites were estimated using the BET equation based on nitrogen adsorption. The Ag and Na contents were determined by inductively coupled plasma (ICP) atomic emission spectrometry, and the water contents were evaluated using thermogravimetric analyses (TGA). To identify the crystalline phase and structure, powder X-ray diffraction (XRD) was performed using a rotating cathode X-ray diffractometer (JEOL JDX3500) at 35 kV and 300 mA with a 2θ–θ step scanning mode and graphite-monochromatized Cu Kα radiation. The morphology was investigated using a transmission electron microscope (TEM) of JEOL JEM4000EX with an accelerating voltage of 400 kV. A microstructural observation was also conducted using a scanning transmission electron microscope ((STEM), HITACHI S-5500) at the accelerating voltage of 30 kV; to this end, both SEM and bright-field STEM images were observed on the same position of the sample.

3. Results and discussion

3.1. Na- and H-magadiites

The results of the chemical analyses by ICP for Na- and H-magadiites obtained are summarized in Table 1 together with their BET surface areas. The chemical analyses revealed that the compositional formula at 40 °C can be described as $H_{0.2}Na_{1.8}Si_{14}O_{29}\cdot7.8H_2O$ and $H_{1.4}Na_{0.6}Si_{14}O_{29}\cdot3.9H_2O$, respectively, for Na- and H-magadiite materials; here, the water contents (the n values) were estimated from the TGA measurements. On the other hand, the BET surface area of Na-magadiite was found to be smaller than that of H-magadiite, which is discussed later in connection with the location of Ag-nanoparticles in the magadiite matrixes.

Table 1
Results of chemical analyses of Na contents by ICP and BET surface areas for Na- and H-magadiites

Material	Na[a] (wt%)	BET surface area[b] (m^2/g)
Na-magadiite	3.97	11.6
H-magadiite	1.47	29.2

[a] The samples were obtained at 40 °C.

[b] Prior to measurements, the samples were dried at 120 °C under vacuum for 2 h.

The XRD profiles of Na- and H-magadiites are shown in Fig. 1. For Na-magadiite, almost all the Bragg reflections can be assigned to those reported for the material due to JCPDS 42-1350. For H-magadiite, while the broadening of the reflection peaks and reduced intensity of the 0 0 l reflections are observed, the profile seems to be substantially similar to that of Na-magadiite. This event indicates that the fundamental interlayer structure of Na-magadiite remains in H-magadiite. The interlayer distances, corresponding to the 0 0 1 reflection, are 15.60 and 15.38 Å for Na- and H-magadiites, respectively. Referring to the water contents of each magadiite (n = 7.8 and 3.9 for Na-

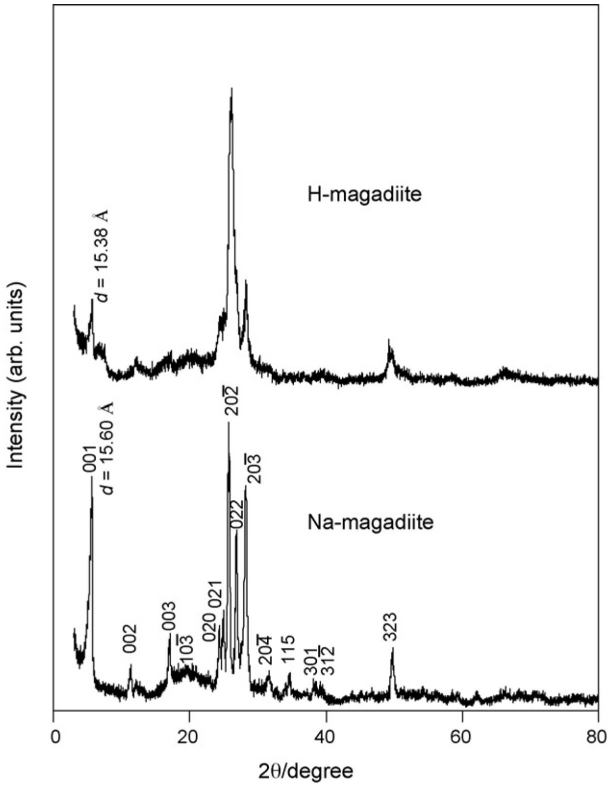

Fig. 1. XRD profiles of Na- and H-magadiite materials.

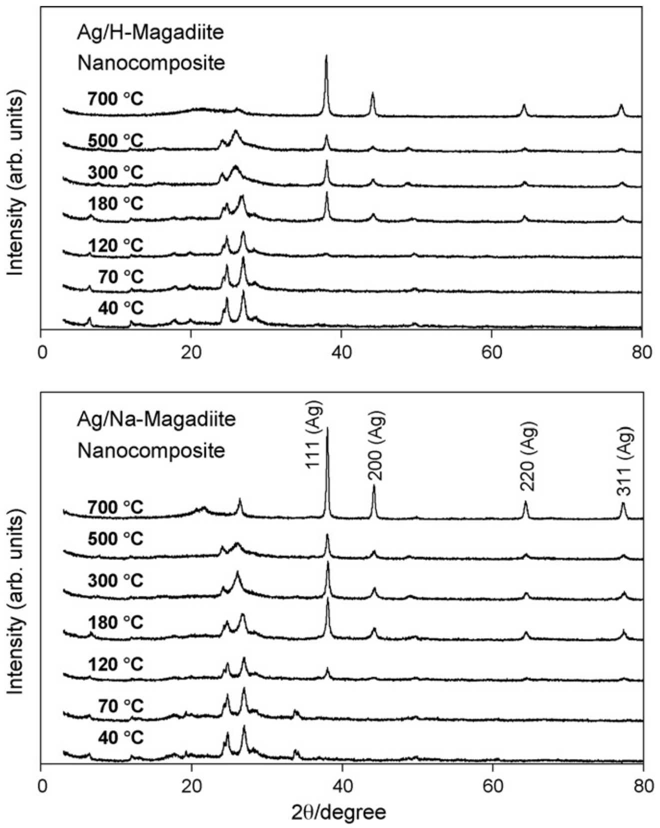

Fig. 2. XRD profiles of Ag-magadiite nanocomposites heated at various temperatures ranging from 40 to 700 °C in air.

and H-magadiites, respectively), these interlayer distances are in good agreement with Eypert–Blaison et al.'s report,[11] in which the interlayer distance in Na-magadiite is shown to be dependent on the number of water molecules (the *n* value) and is ∼15.5 Å for $n \geq \sim 3.5$.

3.2. Ag-magadiite nanocomposites

Fig. 2 shows the XRD profiles of Ag-magadiite nanocomposites heated at various temperatures ranging from 40 to 700° in air. The reflection pattern due to the magadiite material is basically held up to 500 °C for both nanocomposites, which indicates that no apparent structural modifications occur in this temperature range. Furthermore, it should be pointed out that reflections due to metallic silver could be observed at a temperature as low as 120 °C for each nanocomposite. To understand the mechanism for such a low temperature formation of metallic silver, investigations are underway in connection with electron spin resonance (ESR) measurements.[12,13]

Fig. 3 shows the bright-field TEM images of Ag-magadiite nanocomposites heated to 120 °C in air. For both nanocomposites, it was observed that individual Ag-nanoparticles show a relatively uniform particle size of 3–5 nm and are well dispersed in each magadiite matrix. In addition, these Ag-nanoparticles characteristically show a uniform lattice image with no irregularity, as shown in the magnification of Fig. 3(a), indicating that the individual Ag-nanoparticles are single crystalline.

It is worthwhile to discuss the influence of the temperature on Ag-nanoparticles dispersed in the magadiite matrixes. Fig. 4 shows the TEM images of Ag-magadiite nanocomposites after heat treatment at 300 °C in air. For both nanocomposites, in which Ag-nanoparticles smaller that 10 nm are observed, Ag-nanoparticles with a larger particle size of ∼50 nm are simultaneously detected. This observation suggests that Ag-nanoparticles heterogeneously enlarge with an increase in the temperature.

Next, let us further consider the dispersion behavior of Ag-nanoparticles in the magadiite matrixes. Fig. 5 shows typical SEM and STEM images of the Ag-magadiite nanocomposite based on Na-magadiite heated at 180 °C in air; it is noteworthy that, for the SEM and STEM images, the sample was in the same position, and, as a matter of course, the Ag-nanoparticles appear as white and black spherical bodies, respectively, for the SEM and STEM images. In Fig. 5, in addition to Ag-nanoparticles with a particle size of 3–5 nm, Ag-nanoparticles with a slightly larger particle size of ∼10 nm are also observed, which indicates that the heterogeneous enlargement of Ag-nanoparticles occurs when the temperature exceeds ∼180 °C. Furthermore, there is an area in which the number of Ag-nanoparticles in the

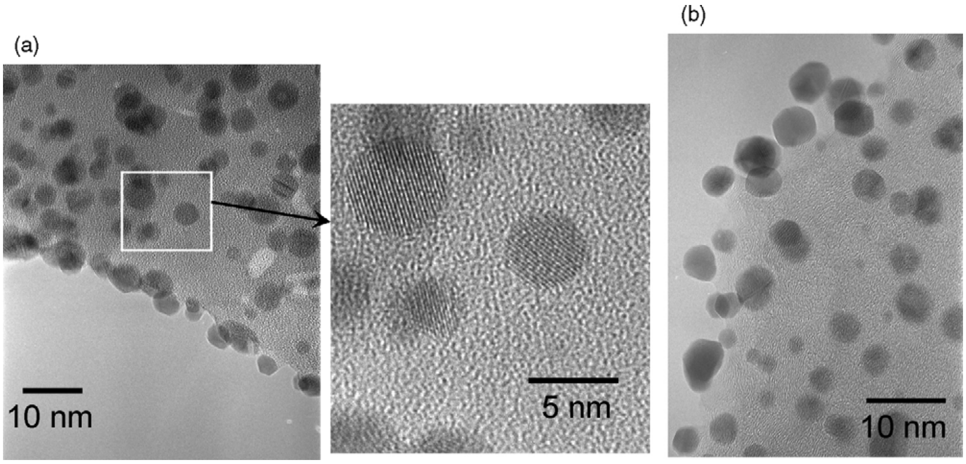

Fig. 3. Bright-field TEM images of Ag-magadiite nanocomposites based on Na-magadiite (a) and H-magadiite (b) heated at 120 °C in air.

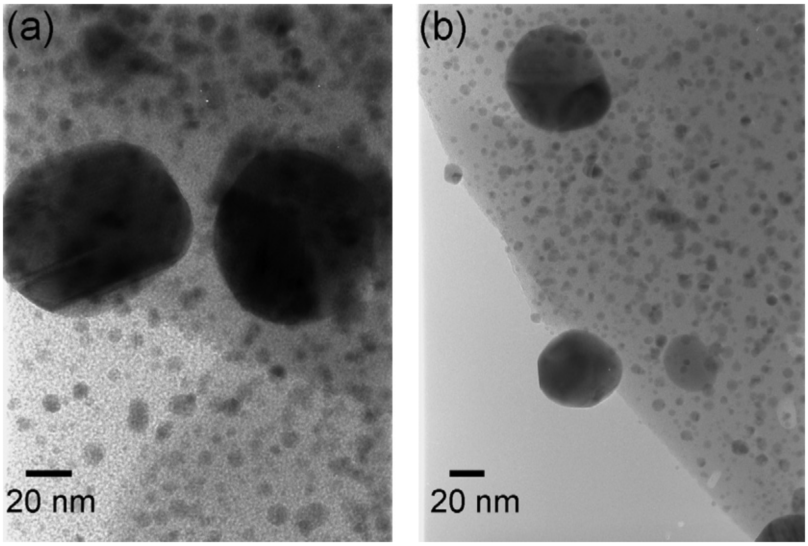

Fig. 4. Bright-field TEM images of Ag-magadiite nanocomposites based on Na-magadiite (a) and H-magadiite (b) after being heated at 300 °C in air.

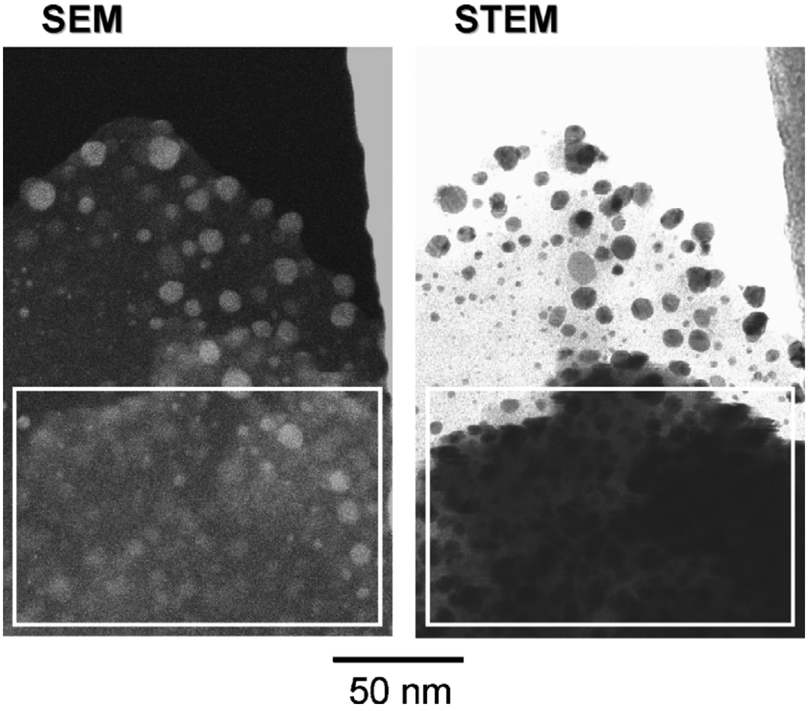

Fig. 5. SEM and STEM images of Ag-magadiite nanocomposite based on Na-magadiite heated at 180 °C in air.

SEM image is considerably decreased compared with that in the STEM image, as shown an area outlined in Fig. 5; it appears that such an area arises from a multilayered structure of the magadiite material. In addition to this observation, the results of Ag contents and BET surface areas, as reported next, suggest that Ag-nanoparticles are mostly located in the interlayer spaces of the magadiite materials.

Table 2 lists the Ag and Na contents of Ag-magadiite nanocomposites at 40 °C. In Table 2, the Ag-content of the Na-magadiite nanocomposite is slightly larger than that of the H-magadiite nanocomposite. In contrast, referring to Table 1, the BET surface area of Na-magadiite is smaller than that of H-magadiite. These results can be understood by considering a location of Ag-nanoparticles such as that discussed above. On the other hand, the Na contents (Table 2) are found to be significantly decreased compared to those in Na- and H-magadiites

Table 2
Results of chemical analyses of Ag and Na contents by ICP for two types of the nanocomposites obtained at 40 °C

Nanocomposite	Ag (wt%)	Na (wt%)
Ag/Na-magadiite	12.03	0.57
Ag/H-magadiite	10.02	0.07

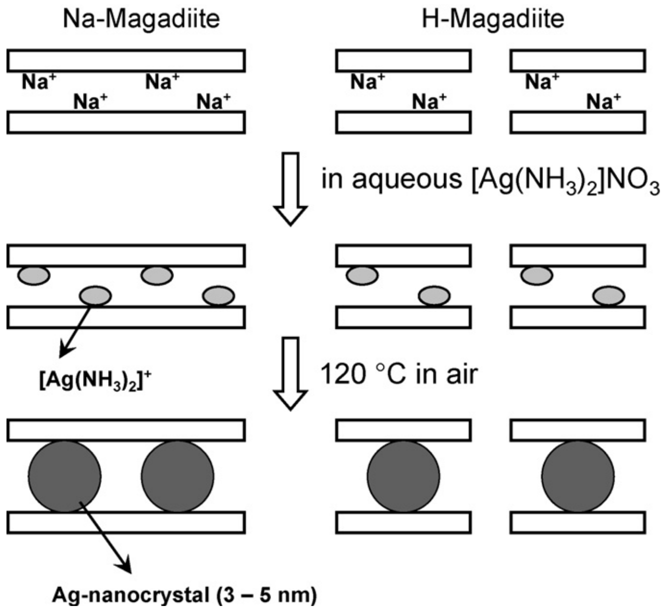

Fig. 6. Schematics illustrating the formation of Ag-nanoparticles in the magadiite matrixes.

(Table 1), which suggests that the Na^+ ions elute during the soaking process, probably due to the ion exchange of Na^+ for $[Ag(NH_3)_2]^+$ and $NH_4{}^+$.

According to the above results, the formation of Ag-nanoparticles in Na- and H-magadiite matrixes could be schematically represented, as shown in Fig. 6. In an aqueous solution, the $[Ag(NH_3)_2]^+$ ions are incorporated into the interlayer spaces of the magadiite materials due to the ion-exchange reaction with the Na^+ ions. Ag-nanoparticles are produced by heating the $[Ag(NH_3)_2]^+$ ions in air at above ~120 °C, and heterogeneous enlargement of the Ag-nanoparticles then occurs when the temperature exceeds ~180 °C.

4. Conclusions

In this paper, we have described the preparation of Ag-magadiite nanocomposites by an ion-exchange method and their structural characterization and morphology. For the nanocomposites, it was found that Ag-nanoparticles with a relatively uniform particle size of 3–5 nm are well dispersed in the interlayer spaces of the magadiite matrixes. These Ag-nanoparticles are formed at a low temperature of ~120 °C and comprised of a single-crystalline particle. Such a dispersion behavior of Ag-nanoparticles would be caused by ion exchange of the $[Ag(NH_3)_2]^+$ with the interlayer Na^+.

It is noteworthy that such Ag-magadiite nanocomposites have a possible use as an efficient catalyst for NO_x reduction,[14] and its preparation method may be applicable to a wide range of systems.

Acknowledgements

The authors are grateful to Takayoshi Tanaka (National Institute for Materials Science, NIMS) for the measurement of the BET surface areas and to Toru Awane (NIMS) for the STEM measurement. We also wish to acknowledge Dr. Hirohisa Yamada (NIMS) and Prof. Jacek Michalik (Institute of Nuclear Chemistry and Technology, Poland) for their participation in helpful scientific discussions. This work was supported by a Grant-in-Aid for Scientific Research from the Ministry of Education, Culture, Sport, Science, and Technology in Japan.

References

[1]. Zhu, H. Y., Orthman, J. A., Li, J.-Y., Zhao, J.-C., Churchman, G. J. and Vansant, E. F., Novel composites of TiO_2 (anatase) and silicate nanoparticles. *Chem. Mater.*, 2002, **14**, 5037–5044.
[2]. Choy, J.-H., Park, J.-H. and Yoon, J.-B., Multilayered SiO_2/TiO_2 nanosol particles in two-dimensional aluminosilicate catalyst-support. *J. Phys. Chem. B*, 1998, **102**, 5991–5995.
[3]. Mogyorósi, K., Dékány, I. and Fendler, J. H., Preparation and Characterization of clay mineral intercalated titanium dioxide nanoparticles. *Langmuir*, 2003, **19**, 2938–2946.
[4]. Miao, S., Liu, Z., Han, B., Zhang, J., Yu, X., Du, J. *et al.*, Synthesis and characterization of TiO_2-montmorillonite nanocomposites and their application for removal of methylene blue. *J. Mater. Chem.*, 2006, **16**, 579–584.
[5]. Eugster, H. P., Hydrous sodium silicates from Lake Magadii, Kenya: precursors of bedded chert. *Science*, 1967, **157**, 1177–1180.
[6]. Lagaly, G., Beneke, K. and Weiss, A., Magadiite and H-magadiite: II. H-magadiite compounds and its intercalation compounds. *Am. Miner.*, 1975, **60**, 650–658.
[7]. Fletcher, R. A. and Bibby, D. M., Synthesis of kenyaite and magadiite in the presence of various anions. *Clays Clay Miner.*, 1978, **35**, 318–320.
[8]. Huang, Y., Jiang, Z. and Schwieger, W., Vibrational spectroscopic studies of layered silicates. *Chem. Mater.*, 1999, **11**, 1210–1217.
[9]. Schwieger, W., Selvam, T., Gravenhorst, O., Pfänder, N., Schlögl, R. and Mabande, G. T. P., Intercalation of $[Pt(NH_3)_4]^{2+}$ ions into layered sodium silicate magadiite: a useful method to enhance their stabilization in a highly dispersed state. *J. Phys. Chem. Solids*, 2004, **65**, 413–420.
[10]. Maeda, M., Maegawa, Y., Yamaguchi, T. and Ohtaki, H., X-ray diffraction studies on the structures of diammine- and aquasilver (I) complexes in aqueous solution. *Bull. Chem. Soc. Jpn.*, 1979, **52**, 2545–2550.
[11]. Eypert-Blaison, C., Sauzéat, E., Pelletier, M., Michot, L. J., Villiéras, F. and Humbert, B., Hydration mechanisms and swelling behavior of Na-magadiite. *Chem. Mater.*, 2001, **13**, 1480–1496.
[12]. Michalik, J., Yamada, H., Brown, D. R. and Kevan, L., Amall silver clusters in smectite caly interlayers. *J. Phys. Chem.*, 1996, **100**, 4213–4218.
[13]. Yamada, H., Michalik, J., Sadlo, J., Perlinska, J., Takenouchi, S., Shimomura, S. *et al.*, Electron spin resonance studies on silver atoms in imogolite fibers. *Appl. Clay Sci.*, 2001, **19**, 173–178.
[14]. Tada, H., Ishida, T., Takao, A., Ito, S., Mukhopadhyay, S., Akita, T. *et al.*, Kinetic and DFT studies on the Ag/TiO_2-photocatalyzed selective reduction of nitrobenzene to aniline. *Chem. Phys. Chem.*, 2005, **6**, 1537–1543.